Article

Not peer-reviewed version

Ixodes scapularis Calreticulin Binds Complement Proteins but Does Not Protect *Borrelia burgdorferi* from Complement Killing

Moiz Ashraf Ansari , Thu-Thuy Nguyen , Klaudia Izabela Kocurek , Tae Heung Kim , Kim Kwon Tae-kwon , Albert Mulenga *

Posted Date: 25 April 2024

doi: 10.20944/preprints202404.1648.v1

Keywords: *Ixodes scapularis;* complement cascade; tick calreticulin; *Borrelia burgdorferi*

 doi:10.20944/preprints202404.1648.v1

Article

Ixodes scapularis Calreticulin Binds Complement Proteins but Does Not Protect *Borrelia burgdorferi* from Complement Killing

Moiz Ashraf Ansari [1], Thu-Thuy Nguyen [1], Klaudia Izabela Kocurek [2], Tae Heung Kim [1], Kim Kwon Tae Kwon [3] and Albert Mulenga [1,*]

[1] Department of Veterinary Pathobiology, School of Veterinary Medicine and Biomedical Sciences, Texas A&M University, College Station, Texas, United States of America
[2] Department of Chemistry, Texas A&M University, College Station, Texas, United States of America
[3] Department of Diagnostic Medicine/Pathobiology, College of Veterinary Medicine, Kansas State University, Manhattan, Kansas, United States of America
* Correspondence: amulenga@cvm.tamu.edu. Tel.: +01-979-458-4300

Abstract *Ixodes scapularis* is a blood-feeding obligate ectoparasite responsible for transmitting the Lyme disease (LD) agent, *Borrelia burgdorferi*. During the feeding process, *I. scapularis* injects *B. burgdorferi* into the host along with its saliva, facilitating the transmission and colonization of the LD agent. Tick calreticulin (CRT) is one of the earliest tick saliva proteins identified and is currently utilized as a biomarker for tick bites. Our recent findings revealed elevated levels of CRT in the saliva proteome of *B. burgdorferi*-infected *I. scapularis* nymphs compared to uninfected ticks. Differential precipitation of proteins (DiffPOP) and LC-MS/MS analyses were used to identify the interactions between *Ixs (I. scapularis)* CRT and human plasma proteins and further exploring its potential role in shielding *B. burgdorferi* from complement killing. We observed that although yeast expressed recombinant (r) *Ixs*CRT binds to the C1 complex (C1q, C1r, and C1s), the activator of complement via the classical cascade, it did not inhibit deposition of the membrane attack complex (MAC) via the classical pathway. Intriguingly, r*Ixs*CRT binds intermediate complement proteins (C3, C5, and C9) and reduces MAC deposition through the lectin pathway. Despite inhibition of MAC deposition in the lectin pathway, r*Ixs*CRT did not protect a serum sensitive *B. burgdorferi* strain (B314/pBBE22*Luc*) from complement-induced killing. As *B. burgdorferi* establishes a local dermal infection before disseminating to secondary organs, it is noteworthy that r*Ixs*CRT promotes the replication of *B. burgdorferi* in culture. We hypothesize that r*Ixs*CRT may contribute to the transmission and/or host colonization of *B. burgdorferi* by acting as a decoy activator of complement and by fostering *B. burgdorferi* replication at the transmission site.

Keywords: *Ixodes scapularis;* complement cascade; tick calreticulin; *Borrelia burgdorferi*

1. Introduction

The black legged tick, *Ixodes scapularis,* is a 3-host tick blood feeding ectoparasite that completes its life cycle (larvae to nymph to adult) over 2 years. This tick is considered endemic to several parts of USA including Midwest, Northeast, West, Southeast, and Southern USA and its distribution is dependent on the various ecological factors such as climates, vegetation, landscape and availability of host [1,2]. *I. scapularis,* which transmits 7 of 16 human tick borne disease (TBD) agents in the USA [2] including causative agents of anaplasmosis (*Anaplasma phagocytophilum*), babesiosis (*Babesia microti*), ehrlichiosis (*Ehrlichia chaffeensis*), hard Tick Relapsing Fever (*Borrelia miyamotoi*), *Powassan encephalitis* virus [3-5], is famously known for transmission of causative agents of Lyme disease (LD): *Borrelia burgdorferi* [6] and the recently described *B. mayonii* [7-9]. LD is among the most important human TBD with ≈476,000 diagnosed cases nationally per year and can cost up to $1 billion without including suspected, undiagnosed and nonacute cases. The accurate economic cost of LD will be much higher if all parameters were included when generating estimates [10]. In the absence of effective vaccines against LD and other TBD agents, killing of ticks using acaricides, personal

 doi:10.20944/preprints202404.1648.v1

protections and avoidance of infected ticks are the only available options to prevent TBD. However, limitations associated with acaricide use such as tick resistance [11], toxicity [12], cost effectiveness [13], and environmental contamination have necessitated the development of alternative tick control methods. Immunization against tick feeding has emerged as the most promising alternative tick control method [14]. Identification and target validation of key tick saliva proteins that facilitate feeding and transmission of TBD agents by ticks is needed before tick antigen-based vaccines to prevent TBD could be developed. Toward this goal, our lab has identified and functionally characterized tick saliva proteins secreted by different stages of ticks and different phases of feeding [15-17]. Recently, we found *I. scapularis* tick calreticulin (*Ixs*CRT) among proteins that were highly secreted by *B. burgdorferi* infected *I. scapularis* nymph [15]. The objective of this study was to characterize the role of *Ixs*CRT as a tick saliva transmission factor of *B. burgdorferi.*

Tick CRT is among highly conserved tick saliva proteins which is found to be expressed universally in all developmental stages and tissues of ticks and has been reported to be secretory protein in saliva of multiple tick species including *Amblyomma americanum, Rhipicephalus microplus* and *I. scapularis* [18-20]. Except for erythrocytes, CRT has been reported in every cell of higher organisms. CRT shows multiple functions including calcium homeostasis, chaperon activity, lytic activity through T and natural killer (NK) cells, boosting the phagocytosis of apoptotic cells, suppressing tumor growth [21,22]. Similarly, tick CRT is also a calcium ion binding protein and it is believed that since calcium ion is an important factor for blood clotting, the tick might be secreting this protein to prevent blood clotting [23]. This concept was explored in another study which showed that *Haemonchus contortus* CRT prevented blood clotting by binding to Ca^{2+} and sequestering blood clotting factors, prothrombin factor X, and C-reactive protein [24,25].

Several studies reported elevated antibodies to tick CRT following tick bites and consequently, tick CRT serves as a biomarker for tick bites [18,26,27]. However, the role(s) of tick CRT in feeding and pathogen transmission is not fully known. Functional analyses of CRT in other parasites including *Trypanosoma cruzi*, *Haemonchus contortus*, *Entamoeba histolytica*, *Trypanosoma carassii* have suggested that parasite CRT blocks the complement cascade by binding with complement component, C1q [21,24,28,29]. In our lab, we previously reported that recombinant *Amblyomma americanum* tick CRT bound C1q, a member of the C1 complex, but did not inhibit deposition of terminal complex of complement cascade [30,31]. Similarly, in this study, we report that yeast expressed recombinant *I. scapularis* CRT (r*Ixs*CRT) binds complement C1 complex proteins (C1q, C1r, and C1s). Although, the C1 complex activates the complement system via classical pathway, r*Ixs*CRT binding of the C1 complex did not inhibit deposition of the membrane attack complex (MAC) in the classical pathway. Interestingly, r*Ixs*CRT also bound intermediate complete system factors, (C3, C5 and C9) and significantly reduced MAC deposition via the lectin pathway. Importantly, while r*Ixs*CRT did not rescue *B. burgdorferi* from complement killing, it promoted the growth of *B. burgdorferi* in culture. Our data suggests that *B. burgdorferi* stimulates the tick to secrete high amounts of CRT that could promote its growth at the tick feeding site.

2. Material and Methods

2.1. Expression and Affinity Purification of Recombinant I. Scapularis Calreticulin (rIxsCRT)

Expression of r*Ixs*CRT was done using pPICZαA and *Pichia pastoris* yeast expression system as previously described [31]. Synthesis of the r*Ixs*CRT expression plasmid was outsourced (Biomatik, Wilmington, DE, USA). The mature protein coding domain was based on *I. scapularis* CRT sequence in GenBank (accession # AY690335.1) with inclusion of a C-terminus hexa-histidine fusion tag and was cloned between *Eco*RI and *Not*I sites in pPICZαA plasmid. The r*Ixs*CRT expression plasmid was used to transform *P. pastoris* (X-33) as described [32]. Transformed colonies were selected on Yeast Extract Peptone Dextrose Medium with Sorbitol (YPDS) agar plates with zeocin (100 µg/mL) incubated at 28°C. Positive transformants (confirmed by PCR check) were inoculated in Buffered Glycerol-complex Medium (BMGY) and grown overnight at 28°C with shaking (230–250 rpm). Subsequently the cells were used to inoculate Buffered Methanol-complex Medium (BMMY) to A_{600}

 doi:10.20944/preprints202404.1648.v1

of 1 after which protein expression was induced by adding methanol up to 1% final concentration every 24 h. Pilot expression showed that expression levels of r*Ixs*CRT peaked at day 3. Thus, for large-scale 1 L cultures, we cultured yeast for up to three days. The pPICZαA plasmid secretes the recombinant protein into media, and thus, r*Ixs*CRT was salted out using ammonium sulfate saturation as described [31]. Precipitated r*Ixs*CRT was dialyzed against column binding buffer (1M NaCl, 0.4M Tris, 0.2M imidazole, pH7.4) and was affinity purified using HiTrap chelating HP column as per the manufacturer's instructions (Cytiva, Marlborough, MA, USA). Expression and affinity purification of r*Ixs*CRT was confirmed by SDS-PAGE and visualized by silver staining and western blotting analysis using antibodies against C-terminus hexa-histidine fusion tag (Thermo Fisher Scientific, Waltham, MA, USA). The affinity-purified r*Ixs*CRT was dialyzed against 10 mM HEPES buffer pH 7.4, 1X PBS pH 7.4 or normal saline based on appropriate assays described below and stored in −80°C until used.

2.2. Differential Precipitation (DIffPOP) of rIxsCRT and Human Plasma Proteins

To identify plasma proteins that might interact with tick saliva CRT, protein-to-protein interaction using differential precipitation was conducted as published [33,34]. Briefly, the reaction volume of 150µl was prepared by preincubating r*Ixs*CRT (10 µg) with 10% Normal Human Serum (NHS) for 90min at 37˚C. NHS only and r*Ixs*CRT only were included as negative controls. After incubation, 100 µL of stabilizing buffer (Phosphoprotein Kit, Buffer A, Takara Bio Company, CA, USA) was added to the reaction. Subsequently, to fractionate, an escalating amount of precipitation buffer (90% methanol/1% acetic acid) starting at 3.75 µL (or 0.9% of reaction volume) in fraction 1 to 317 µL (or 79.25% of reaction) in fraction 10 was added to the reaction mixture (Supplemental Table S1) followed by vortexing to mix. The reaction was incubated at RT (room temperature) for 5 min and centrifuged at 13000xg for 10 min at 4˚C. The supernatant was carefully transferred to another tube without disturbing the pellet and transfer to another 1.5 mL centrifuge tube and repeated the precipitation process for 9 more times. The collected pellets (n=10) were washed with ice cold acetone, airdried, and dissolved in PBS and considered as fractions 1-10. The plasma proteins that interacted with r*Ixs*CRT were expected to co-precipitate with r*Ixs*CRT. Subsequently, each fraction was resolved on 10% SDS-PAGE gel, silver stained, and subjected to the standard western blot analysis using antibodies to the hexa-histidine tag to track r*Ixs*CRT fractionation. To identify plasma proteins that interacted with r*Ixs*CRT, fractions were subjected to LC-MS/MS analysis.

2.3. LC-MS/MS Analysis

The samples for LC-MS/MS analysis were prepared by in-solution protein digestion method. In this method, 10 µg of differentially fractionated proteins were acetone precipitated and reconstituted in 100 µL of digestion buffer (50 mM ammonium bicarbonate in water, pH 8.5) and reduced with DTT (2 mM). The solution was incubated at 60˚C for 30 min and then alkylated with 10 mM of iodoacetamide and incubated in dark for 30 min at 60˚C. Subsequently, proteins were digested overnight at 37˚C with trypsin at 50:1 ratio (protein-to-trypsin) and submitted for LC-MS/MS analysis. LC-MS/MS analysis was performed on the Thermo Scientific Orbitrap Fusion tribrid mass spectrometer equipped with a Dionex UltiMate 3000 reverse-phase nano-UHPLC system. 1 µl of each sample was injected onto and separated by a 150 × 0.075 mm C18 column (Phenomenex bioZen XB-C18, 2.6 µm particle size) at a flow rate of 0.400 µl/min. The total duration of the method was 60 minutes, with the gradient as follows: equilibration at 2% B (98% acetonitrile, 2% water, 0.1% formic acid), ramp to 45% B at 37 minutes, ramp to 90% B at 40 minutes and hold until 46 minutes, ramp down to 2% B at 47 minutes and hold at 2% B until the end of the run at 60 minutes.

Eluent was introduced into the Fusion mass spectrometer by nano-ESI at a static voltage of 2450 V, with a transfer capillary temperature of 275 °C. Mass spectrometry data were acquired in positive mode at a resolution of 120,000 (at m/z 200) in the m/z range 400-1600. The RF lens was set to 60%. Maximum injection time was 100 ms. Scans were acquired in top speed mode with a cycle duration set to 3 seconds. The intensity threshold for precursors of interest was 5.0e3. Charge states 1-6 were considered. Dynamic exclusion was set to 60 seconds with a mass tolerance of 10 ppm. MS/MS data

 doi:10.20944/preprints202404.1648.v1

were acquired by HCD at a fixed collision energy of 28% with a precursor ion isolation window of 1.6 m/z; fragments were detected in the ion trap at a rapid scan rate. Proteome Discoverer 2.4 software (Thermo Fisher Scientific, Waltham, MA, USA) was used to analyze the MS/MS spectra of peptide ions to search against the publicly available NCBI protein database (www.ncbi.nlm.nih.gov). Plasma protein and r*Ixs*CRT interactions were confirmed if the normalized spectral abundance factor was significantly different between controls (plasma only) and treatment (plasma and r*Ixs*CRT) treatments.

Subsequently, the pathways that were represented by interactions between r*Ixs*CRT and plasma proteins were revealed on the Reactome database (http://reactome.org) [35]. Accession numbers of plasma protein interactors with r*Ixs*CRT were loaded onto the Reactome database server and highly significant pathways were reported.

2.4. Pull-Down Assays to Validate Interactions between rIxsCRT and Human Complement Proteins

Prompted by DiffPOP and LC-MS/MS analyses interactions between complement proteins and r*Ixs*CRT, Dynabeads™ His-Tag Isolation and Pulldown magnetic beads (Thermo Fisher Scientific, Waltham, MA, USA) was used to perform the pull-down assay to validate interactions. The experiment was performed according to manufacturer's guidelines with minor modifications. Briefly, 50 µL (2 mg) of magnetic Dynabeads™ was transferred to 1.5 mL microcentrifuge tube and placed on the magnetic stand for 2 min and the supernatant was discarded. Purified r*Ixs*CRT (40 µg) was added to the beads and briefly vortexed to mix. The mixture was incubated on a roller at RT for 2 h. The tube was placed on the magnet for 2 min and supernatant was discarded. To remove nonspecific interactions, the beads were washed 4 times with the washing buffer (100 mM Sodium Phosphate (pH 8), 600 mM NaCl, 0.02% Tween-20). The test proteins, human complement serum (HCS; Innovative Research, Inc, Novi, MI, USA) were diluted to 10% in the pull-down buffer (6.5 mM Sodium phosphate pH 7.4, 140 mM NaCl, 0.02% Tween-20) and were added to the bead-bait complex and incubated on a roller for 2 h at RT. Then, the mixture was placed on the magnetic stand for 2 min and the supernatant was discarded. The beads were washed 4 times with the wash buffer (100 mM sodium phosphate, pH 8.0, 600mM NaCl, 0.02% Tween-20) and test protein complex were eluted by incubating the beads with elusion buffer (300mM Imidazole, 50mM Sodium phosphate pH 8.0, 300mM NaCl, 0.01% Tween-20) for 5min at RT. Subsequently, eluted proteins were subjected to standard SDS-PAGE and western blot analysis using antibodies to specific complement proteins: C1q (Thermo Fisher Scientific, Waltham, MA, USA), C1r (Thermo Fisher Scientific, Waltham, MA, USA) and C1s (Sino Biological, Inc., Houston, TX, USA); Activated C3 Antibody (I3/15) (Santa Cruz Biotechnology, Inc. Dallas, TX, USA), inactive C3 (Complement Technology, Inc., Tyler, TX, USA), C5 (Complement Technology, Inc., Tyler, TX, USA), C9 (Complement Technology, Inc., Tyler, TX, USA), and the C5-9 complex or membrane attack complex: MAC (Santa Cruz Biotechnology, Inc. Dallas, TX, USA). For controls, r*Ixs*CRT only and HCS only samples were processed.

2.5. ELISA Analysis to Validate rIxsCRT Binding of Complement Proteins

Preliminary differential precipitation and pulldown assays showed that r*Ixs*CRT likely interacted with complement proteins. To further substantiate these interactions, conventional ELISA was used. High Binding plates (Thermo Fisher Scientific, Waltham, MA, USA) were coated with r*Ixs*CRT (250 ng) in ELISA coating buffer (carbonate-bicarbonate buffer, pH 9.6) overnight at 4°C. Subsequently, wells were washed 3 times with phosphate buffer saline with Tween 20 (PBST) and the non-specific binding sites were blocked using blocking buffer (5% skim milk dissolved in PBST) for 2 h at RT. Following washing, 10% normal human serum (NHS) was added to the wells and was incubated for 2 h at RT. The coated plate was washed with PBST and wells were incubated for 3 h with respective primary polyclonal antibodies (Anti-C1q, Anti-C1r, Anti-C1s) and anti-sera (Anti-C3, Anti-C5 and Anti-C9) to complement proteins, at 1:5000 dilution. Wells were washed 3 times with PBST and incubated with respective HRP conjugated secondary antibody for 1 h (Anti-Rabbit for C1q, C1r and C1s, and anti-Goat for C3, C5 and C9). Wells were again washed 3 times with PBST, and bound peroxidase activity was observed by adding 1-Step Ultra TMB-ELISA substrate (Thermo

 doi:10.20944/preprints202404.1648.v1

Fisher Scientific, Waltham, MA, USA) and reaction was stopped using 2M sulfuric acid. The intensity of color development was quantified by measuring intensity at 450nm using microplate reader (Biotek Instrument Inc., Winooski, VT, USA).

2.6. Effect of rIxsCRT on Complement Activation

The effects of r*Ixs*CRT of complement activation was assayed using the Wieslab® Complement System Screen (Svar Life Science AB, Malmo, Sweden) according to the manufacturer's recommendation and as previously published [34,36]. This kit evaluates effects on membrane attack complex (MAC) deposition via each of the three complement system activation pathways: Classical, Lectin, and Alternative. To test the effect of the r*Ixs*CRT on the complement pathways, NHS (provided with the kit) was diluted according to the manufacturer's instructions and incubated at RT for 15 min. Briefly, r*Ixs*CRT (4 µM), was added to the NHS and incubated at 37°C for 30min, before adding the samples to the wells of the Wieslab® plates. The 100 µL of r*Ixs*CRT and NHS samples (provided in the kit) were then added to the wells of the Wieslab® plates along with positive control (human serum, provided with kit, negative controls (provided with kit) and blank (diluent only) in duplicates, and incubated at 37°C for 1 h. Finally, absorbance was read at 405 nm on a Biotek Synergy H1 microplate reader (Biotek Instrument Inc., Winooski, VT, USA). The MAC deposition rate was calculated as follows: (Sample-NC)/(PC-NC) x100 where NC is negative control and PC is positive control.

2.7. Complement Sensitivity Assay

Our preliminary findings shows that r*Ixs*CRT dose dependently reduced deposition of the MAC by mannose-binding lectin pathway, so we were interested to study its effect to rescue complement sensitive *B. burgdorferi* spirochete. The complement sensitive *B. burgdorferi* (B314/pBBE22*Luc*) and resistant (B314/pCD100) strains [37] were a kind gift from Jon. T. Skare laboratory (Texas A&M University Health Science Center, College Station, TX, USA). Both strains were maintained in BSK-II media supplemented with 6% rabbit serum at 32°C, 1% CO_2 for this assay. 15 µL of normal human serum (NHS) (Complement Technology, Inc., Tyler, TX, USA) was pre-incubated with serial dilutions of r*Ixs*CRT (0.25, 0.5, 0.75, and 1µM) at 37°C for 30 min prior to addition of 85 µl of *B. burgdorferi* B314/pBBE22*luc* (10^6 cells/ml) and inoculated in a bio-shaker at 32°C with shaking at 100 rpm, PBS (Phosphate buffered saline) was used as blank. NHS with *B. burgdorferi* B314/pBBE22*luc* and B314/pPCD100 were included as negative and positive controls respectively. Survival of spirochetes was assessed at 1.5 h, 2 h, 2.5 h and 3 h post incubation. Spirochetes were counted from randomly chosen fields (10-15 fields) under a dark-field microscope. Spirochete viability was arbitrated based on cell mobility, membrane integrity, and cell lysis as described elsewhere [37]. Spirochete survival rates were calculated from 3 biological replicates. Heat-inactivated NHS (hiNHS) was used as the no complement-activity control.

2.8. Blood Recalcification Time Assay

To assess the effect of r*Ixs*CRT on blood clotting, the blood recalcification time was calculated as described elsewhere [38,39]. In this assay, normal blood plasma, Pacific Hemostasis™ Coagulation Reference Plasma (Thermo Fisher Scientific, Waltham, MA, USA) was used to measure the recalcification time in the presence of r*Ixs*CRT. In this assay, 50 µl of plasma was incubated with tris-buffer (20mM Tris-HCl, pH 7.5), and r*Ixs*CRT (2.6 mM) at room temperature for 30 min. Simultaneously, 150mM $CaCl_2$ was incubated at 37°C for 30 min. After incubation, plasma with r*Ixs*CRT (140 µL total volume) along with prewarmed $CaCl_2$ (10µL) was placed in triplicate (for each sample) in microwell plate and the absorbance was measured at 650 nm wavelength for 30min at 55 seconds interval. Sample without r*Ixs*CRT was used as positive control and tris-buffer only was used as blank.

 doi:10.20944/preprints202404.1648.v1

2.9. Assessing the Effect of rIxsCRT on B. burgdorferi Growth in In-Vitro Culture

To gauge insight on effect of *Ixs*CRT on *B. burgdorferi*, low passaged (<6 passages) *B. burgdorferi* sensu stricto B31 (strain MSK5) was co-cultured with empirically determined r*Ixs*CRT (2.6 mM) final concentration in BSK-H medium (Sigma-Aldrich, MO, USA) supplemented with 6% rabbit serum. Spirochetes were monitored each day under dark field microscopy to observe any morphological changes. Using the Petroff-Hausser Hemacytometer (Hausser Scientific Co., PA, USA), the starting concentration of *B. burgdorferi* was adjusted to 10^5 cells/ml. From each 5ml culture tube, 5 µL of BSK-H medium was pipetted on a Petroff-Hausser Hemacytometer (Hausser Scientific Co., PA, USA) and the cells were counted in all cells. The number of spirochetes were determined by using following formula: Spirochetes/mL = Average of spirochetes counted in all wells x Dilution factor x 50000 (50,000 = 50 (cell depth is 1/50) X 1000 (1000 cubic mm = 1 milliliter).

To quantify *B. burgdorferi* 200 µL of cells were aliquoted from the culture on day 0, 2, 5 and 7. Genomic DNA (gDNA) for each aliquot were extracted by using the DNeasy Kit according to manufacturer`s instructions (Qiagens, USA). The DNA concentration was determined by Nanodrop (Thermo Fisher Scientific, Waltham, MA, USA). In triplicate, gDNA (500ng) was mixed with empirically determined 300 nM *Fla*B qPCR primers (sense TCTTTTCTCTGGTGAGGGAGCT, anti-sense TCCTTCCTGTTGAACACCCTCT) and the PowerUp SYBR® Green Supermix (Thermo Fisher Scientific, Waltham, MA, USA) in 20 µL reaction volume and subjected to cycling on iQ5 Multicolor Real-Time PCR Detection System (Bio-Rad). *B. burgdorferi* was quantified by comparative analysis using BioRad CFX Maestro 3.2v software which analyzes the Ct values between the standards (10^1, 10^2, 10^3, 10^4, 10^5, 10^6, 10^7, 10^8 cells/ml *B. burgdorferi*) and the test cultures (without treated and r*Ixs*CRT treated *B. burgdorferi*). *Borrelia* count was calculated by plotting the standard curves of Ct values versus the log of copy numbers included in each PCR run [40].

2.10. Identifying the Reaction Intensity of rIxsCRT against B. burgdorferi Infected Rabbit IgG

To ascertain the reactivity of r*Ixs*CRT towards *B. burgdorferi*-infected rabbit IgG, both ELISA and western blot assays were conducted. The ELISA and western blot were performed following the similar steps as mentioned above. For both the assays, 40µg/ml of pre-infested (PI), *B. burgdorferi* infected and uninfected rabbit IgG, was used as primary antibody and anti-Rabbit IgG-HRP conjugated (Southern Biotech, Birmingham, AL, USA) was used as secondary antibody (1:10^4 dilution). Primary antibody used in these assays was purified from the rabbit serum which was infested once with *B. burgdorferi* infected and uninfected *I. scapularis*. The IgG was purified using Protein A/G column (Cytiva, Marlborough, MA, USA) by following the company's instructions.

2.11. Statistical Analysis

To evaluate statistical significance, the data was analyzed using GraphPad Prism 9 software (GraphPad Software Inc., La Jolla, CA, USA) which was represented as mean ± SEM (standard error of the mean) with statistical significance ($P < 0.05$) detected by using the non-parametric Student's t-test and two-tailed ANOVA to 95% confidence interval.

3. Results

3.1. Differential Precipitation of Proteins (DiffPOP) and LC-MS/MS Analyses Reveal Multiple Interactions between rIxsCRT Human and Plasma Proteins

Recombinant (r) *Ixs*CRT was successfully expressed in *P. pastoris* (Figure 1). Affinity purified r*Ixs*CRT migrated at the expected molecular weight size (47.61 kDa) as shown by silver staining (Figure 1A) and western blotting analyses using antibodies to the histidine fusion tag (Figure 1B).

 doi:10.20944/preprints202404.1648.v1

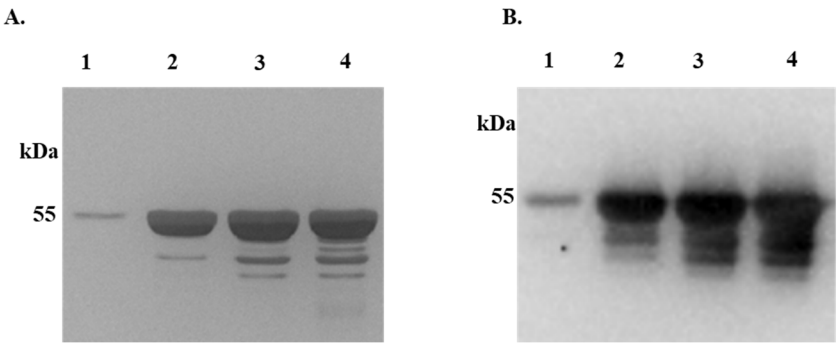

Figure 1. Expression and affinity purification of recombinant *I. scapularis* calreticulin. Recombinant *I. scapularis* calreticulin (r*Ixs*CRT) with His-tag was expressed in *Pichia pastoris* over 3 days and affinity purified under native conditions. Affinity purification of r*Ixs*CRT was validated by standard SDS-PAGE followed by silver staining (A) and western blotting using the antibody to the Histidine fusion tag (B). Lanes 1-4 represents the 50, 75, 100 and 200 imidazole concentration (mM) at which the r*Ixs*CRT was eluted, dialyzed in PBS, concentrated, and were used for the assays.

We previously reported that although *A. americanum* tick CRT bound the C1q complement protein, it did not inhibit activation of classical complement cascade [31]. To expand on these findings, we employed DiffPOP (Figure 2) assay [33]. In this assay, plasma proteins that interacted with r*Ixs*CRT co-precipitated with r*Ix*CRT and western blotting analysis using the antibody to the histidine tag identified co-precipitating fractions 1-8 (Figure 2C). These fractions were subjected to LC-MS/MS analysis and were divided into groups as, pooled lanes 1-5 (hereafter called group A), lane 6 (hereafter called group B), and pooled lanes 7 and 8 (hereafter called group C) to identify the plasma proteins that interacted with r*Ixs*CRT.

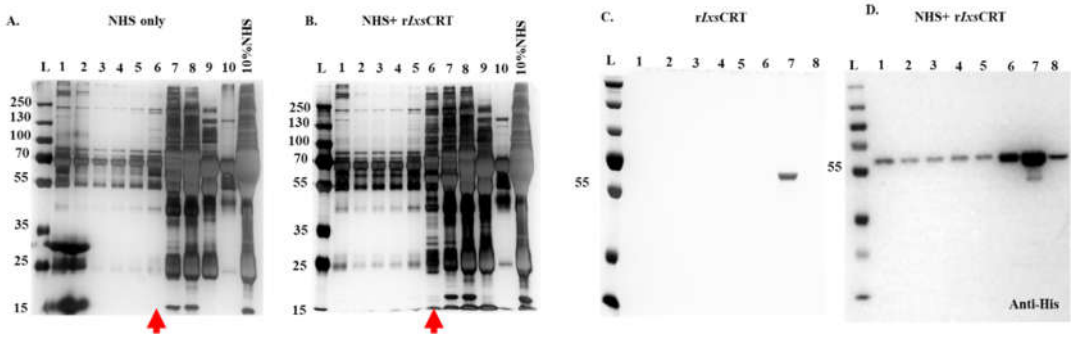

Figure 2. Differential Precipitation of Proteins (DiffPOP) reveals interactions between r*Ixs*CRT and complement proteins. Affinity-purified r*Ixs*CRT (10 µg) was pre-incubated with 10% normal human serum (NHS) for 90 minutes at 37˚C, while NHS and r*Ixs*CRT served as controls. The reactions were then stabilized and subjected to differential precipitation using escalating amount of precipitating buffer as described in the materials and methods (see supplemental Table 1). Different fractions obtained from the precipitation process were analyzed by standard SDS-PAGE and silver staining. Figure 2A shows the protein profile of NHS only, Figure 2B illustrates the profile of NHS + r*Ixs*CRT mixture, and Figure 2C displays the profile of r*Ixs*CRT only. Additionally, the NHS + r*Ixs*CRT mixture was subjected to western blotting analysis using an antibody against the histidine fusion tag to track the precipitation of r*Ixs*CRT (Figure 2D). The distinct protein profile between NHS and NHS + r*Ixs*CRT, highlighted by the red arrowhead in Panels A and B, indicates potential interactions between r*Ixs*CRT and specific proteins. The precipitation profile depicted in Figure 2D guided the selection of fractions for subsequent LCMS/MS analysis, shedding light on the specific complement proteins interacting with r*Ixs*CRT. L: Ladder depicting molecular weight (kDa), Lanes 1-10 = DiffPOP fractions 1-10.

Normalized abundance values were used to construct a volcano plot (Figure 3) as graphical representation of differential co-precipitation of human proteins without or with r*Ixs*CRT. Analysis

 doi:10.20944/preprints202404.1648.v1

of abundance values identified 1074, 1617, and 1936 unique proteins that interacted with r*Ixs*CRT in groups A-C respectively (Supplemental tables S2-S4). To gain further insights, plasma proteins that were detected at least 1.5 folds higher in r*Ixs*CRT and plasma reactions compared to plasma only control were subjected to reactome analysis (Table 1 and Supplemental table S5).

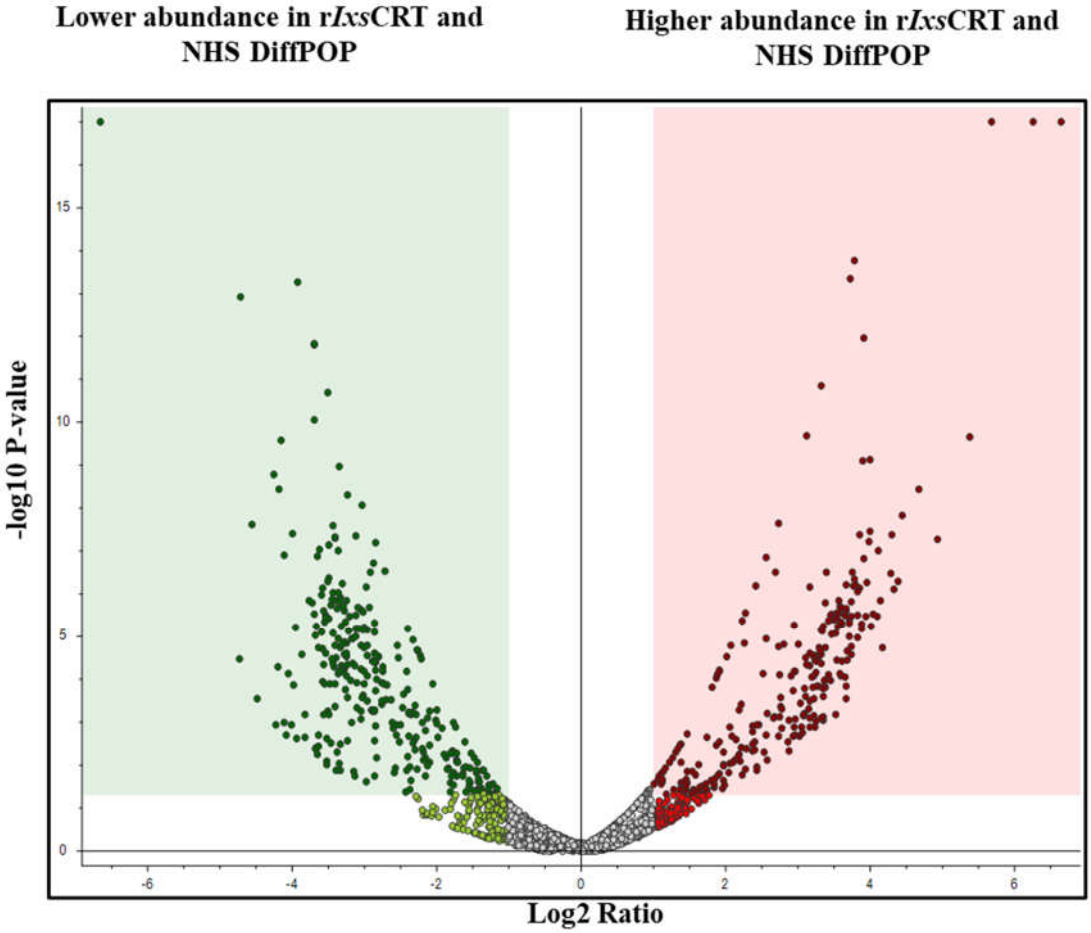

Figure 3. Volcano plot analyses reveal human serum proteins that differentially co-precipitated with r*Ixs*CRT. Normalized abundance values of three biological replicates were used in Proteome Discoverer™ Software (Thermo Fisher Scientific, Tx, USA) to generate the volcano plot. In volcano plot, the Y-axis shows -log10 p-value and X-axis shows magnitude of change (log2 fold change). Red dots represent proteins that co-precipitated in high amounts with r*Ixs*CRT while green dots represent that were absent or co-precipitated in low amounts in presence of r*Ixs*CRT. The adjusted p-value ≤ 0.05 and fold change log2 of more than 2 was used as cut off to select proteins that co-precipitated in high amounts with r*Ixs*CRT.

Table 1. Reactome analysis depicting the pathways linked with proteins which are abundant ≥1.5-fold in NHS treated with CRT.

	Pathway name (reactome identifier)	Entities				Reactions	
		found	ratio	p-value	FDR*	found	ratio
Fraction 1-5	Terminal pathway of complement (R-HSA-166665.4)	2 / 8	6.88e-04	0.009	0.578	4 / 5	3.49e-04
	Defective ABCA12 causes ARCI4B (R-HSA-5682294.3)	1 / 1	8.60e-05	0.017	0.578	1 / 1	6.99e-05

 doi:10.20944/preprints202404.1648.v1

	Defective ABCC2 causes DJS (R-HSA-5679001.4)	1 / 1	8.60e-05	0.017	0.578	1 / 1	6.99e-05
	Regulation of Complement cascade (R-HSA-977606.6)	6 / 135	0.012	0.03	0.578	20 / 42	0.003
	CD22 mediated BCR regulation (R-HSA-5690714.3)	4 / 70	0.006	0.033	0.578	3 / 4	2.80e-04
	Recycling of bile acids and salts (R-HSA-159418.4)	2 / 18	0.002	0.039	0.578	2 / 17	0.001
	Complement cascade (R-HSA-166658.5)	6 / 146	0.013	0.041	0.578	33 / 72	0.005
	Defective factor XII causes hereditary angioedema (R-HSA-9657688.2)	1 / 3	2.58e-04	0.05	0.578	2 / 2	1.40e-04
	Defective SERPING1 causes. hereditary angioedema (R-HSA-9657689.2)	1 / 3	2.58e-04	0.05	0.578	1 / 3	2.10e-04
Fraction 6	Terminal pathway of complement (R-HSA-166665.4)	4 / 8	6.88e-04	9.00e-06	0.004	5 / 5	3.49e-04
	Regulation of Complement cascade (R-HSA-977606.6)	9 / 135	0.012	3.14e-04	0.064	13 / 42	0.003
	Complement cascade (R-HSA-166658.5)	9 / 146	0.013	5.50e-04	0.075	22 / 72	0.005
	Response to elevated platelet cytosolic Ca2+ (R-HSA-76005.3)	7 / 133	0.011	0.005	0.429	2 / 14	9.79e-04
	Regulation of Insulin-like Growth Factor (IGF) transport and uptake by Insulin-like Growth Factor Binding Proteins (IGFBPs) (R-HSA-381426.3)	6 / 124	0.011	0.014	0.61	2 / 14	9.79e-04
	Platelet degranulation (R-HSA-114608.4)	7 / 128	0.011	0.004	0.429	2 / 11	7.69e-04
	Dissolution of Fibrin Clot (R-HSA-75205.4)	2 / 13	0.001	0.018	0.61	15 / 21	0.001
	Post-translational protein phosphorylation (R-HSA-8957275.2)	5 / 107	0.009	0.027	0.61	1 / 1	6.99e-05
	Other semaphoring interactions (R-HSA-416700.2)	2 / 19	0.002	0.036	0.61	3 / 9	6.29e-04
	Sema4D induced cell migration and growth-cone collapse (R-HSA-416572.4)	2 / 20	0.002	0.04	0.61	4 / 7	4.89e-04

 doi:10.20944/preprints202404.1648.v1

	RHO GTPases activate CIT (R-HSA-5625900.3)	2 / 20	0.002	0.04	0.61	3 / 6	4.19e-04
	Common Pathway of Fibrin Clot Formation (R-HSA-140875.5)	2 / 22	0.002	0.047	0.61	6 / 29	0.002
Fraction 7-8	Collagen chain trimerization (R-HSA-8948216.4)	8 / 44	0.004	1.24e-04	0.091	7 / 28	0.002
	Collagen degradation (R-HSA-1442490.4)	8 / 64	0.006	0.001	0.331	11 / 34	0.002
	Anchoring fibril formation (R-HSA-2214320.4)	4 / 15	0.001	0.002	0.331	4 / 4	2.80e-04
	Collagen biosynthesis and modifying enzymes (R-HSA-1650814.5)	8 / 67	0.006	0.002	0.331	30 / 51	0.004
	Integrin cell surface interactions (R-HSA-216083.5)	9 / 85	0.007	0.002	0.331	11 / 55	0.004
	TRKA activation by NGF (R-HSA-187042.2)	2 / 3	2.58e-04	0.005	0.551	4 / 4	2.80e-04
	Collagen formation (R-HSA-1474290.4)	8 / 90	0.008	0.011	0.763	39 / 77	0.005
	NCAM1 interactions (R-HSA-419037.2)	5 / 42	0.004	0.013	0.763	1 / 10	6.99e-04
	ECM proteoglycans (R-HSA-3000178.5)	7 / 76	0.007	0.014	0.763	7 / 23	0.002
	Assembly of collagen fibrils and other multimeric structures (R-HSA-2022090.4)	6 / 61	0.005	0.016	0.763	9 / 26	0.002
	Laminin interactions (R-HSA-3000157.3)	4 / 30	0.003	0.018	0.763	4 / 15	0.001
	Degradation of the extracellular matrix (R-HSA-1474228.5)	10 / 140	0.012	0.019	0.763	13 / 105	0.007
	Crosslinking of collagen fibrils (R-HSA-2243919.4)	3 / 18	0.002	0.022	0.763	1 / 13	9.09e-04
	Activation of TRKA receptors (R-HSA-187015.3)	2 / 7	6.02e-04	0.023	0.763	8 / 8	5.59e-04
	Defective SLC2A9 causes hypouricemia renal 2 (RHUC2) (R-HSA-5619047.3)	1 / 1	8.60e-05	0.032	0.763	1 / 1	6.99e-05
	Role of second messengers in netrin- 1 signaling (R-HSA-418890.2)	2 / 10	8.60e-04	0.043	0.763	1 / 4	2.80e-04

 doi:10.20944/preprints202404.1648.v1

Signaling by PDGF (R-HSA-186797.5)	5 / 60	0.005	0.049	0.763	1 / 31	0.002

* FDR: False Discovery Rate.

Group A (pooled fractions 1-5) proteins mapped to nine pathways (Table 1) that included 3 complement function pathways, the initial triggering of complement cascade, regulation of complement cascade, and terminal pathway of complement (Table 1). Group A proteins were identified as defective ABCA12 (ATP-binding cassette sub-family A member 12) which causes ARCI4B (autosomal recessive congenital ichthyosis 4B) that is associated with reduced protease regulation and skin-barrier dysfunction [41-44], defective ABCC2 (ATP binding cassette subfamily 2) that causes DJS (Dubin–Johnson syndrome) associated with hyperbilirubinemia [45]. Other group A proteins mapped to pathways of defective factor XII and defective SERPING1 which cause hereditary angioedema [46], CD22 (receptor predominantly restricted to B cells) mediated BCR (B-cell receptors) regulation, and recycling of bile acids and salts [47].

Group B (fraction 6) proteins mapped to 12 pathways (Table 1) that included terminal pathway of complement, regulation of Complement cascade, and complement cascade. The other pathways associated with group B proteins include response to elevated platelet cytosolic Ca^{2+}, regulation of Insulin-like Growth Factor (IGF) transport and uptake by Insulin-like Growth Factor Binding Proteins (IGFBPs), platelet degranulation, dissolution of Fibrin Clot, post-translational protein phosphorylation, semaphorin interactions, sema4D induced cell migration and growth-cone collapse, RHO GTPases activate CIT, and Common Pathway of Fibrin Clot Formation.

Finally, group C (pooled fraction 7 and 8) proteins mapped to 17 pathways (Table 1) associated with signaling, extracellular matrix (ECM), and cell adhesion functions. The signaling related pathways include the NGF (nerve growth factor) activated Trk (neurotrophin receptor), netrin-1 signaling which leads to release of intracellular calcium [48] and signaling by PDGF (*platelet*-derived growth factor) associated with cellular immune response [49]. The ECM related pathways include multiple collagen related functions including collagen chain trimerization, biosynthesis, formation, assembly, crosslinking, and degradation. The other ECM functions that mapped group C proteins include anchoring fibril formation, degradation of ECM, and laminin interactions.

3.2. rIxsCRT and Complement Protein Interactions Validated by Western Blotting and ELISA Analyses

Relative abundance analysis revealed that complement proteins co-precipitated at high levels in presence of r*Ixs*CRT as revealed by normalized spectral abundance (Figure 4A and 4B). To validate these findings, all DiffPOP fractions (Figure 2) were subjected to western blotting analysis using antibodies to complement proteins including C1q, C1r, C1s, C3 (inactive and activated), C5, C9, and C5b-9 (or membrane attack complex). This analysis confirmed our differential precipitation and LC-MS/MS analyses data (Figure 3 and 4) as indicated by high protein band intensity of complement proteins that co-precipitated with r*Ixs*CRT compared to NHS only (red arrowhead marked in Figs 5A-5L). Our data also show r*Ixs*CRT bound all three subunits of the complement complex 1 (C1q, C1r, and C1s) along with the C3, C5, and C9 (Figure 5A to 5L).

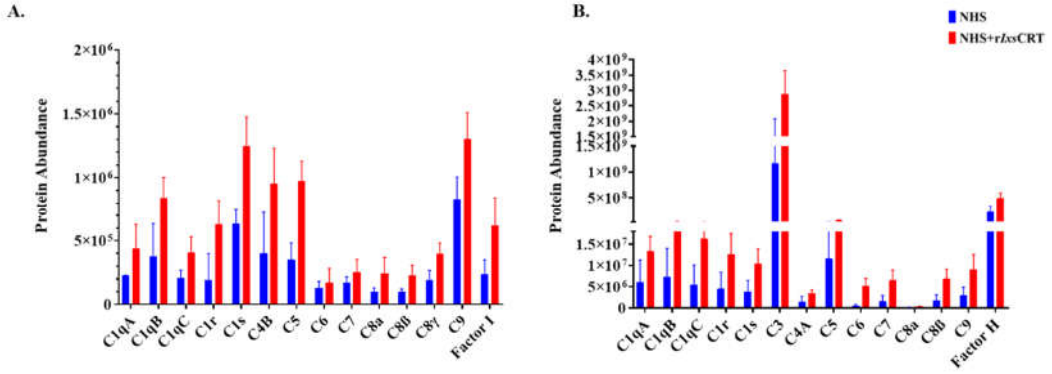

 doi:10.20944/preprints202404.1648.v1

Figure 4. Differential precipitation of complement proteins in the presence of r*Ixs*CRT. Fractions obtained from the Differential Precipitation (DiffPOP) were pooled into group A (fractions 1-5), group B (Fraction 6), and group C (fractions 7 and 8). These fractions were subjected to Liquid Chromatography-Mass Spectrometry (LCMS/MS) analysis to investigate the abundance of complement proteins interacting with r*Ixs*CRT. Figure 4A illustrates the abundance of complement proteins interacting with r*Ixs*CRT in Group A, while Figure 4B depicts the corresponding interactions in Group B. The Y-axis in Figure 4A and 4B illustrates the protein abundance, indicating the levels of proteins co-precipitated with r*Ixs*CRT (depicted by the red graph) in comparison to NHS only (represented by the blue graph).

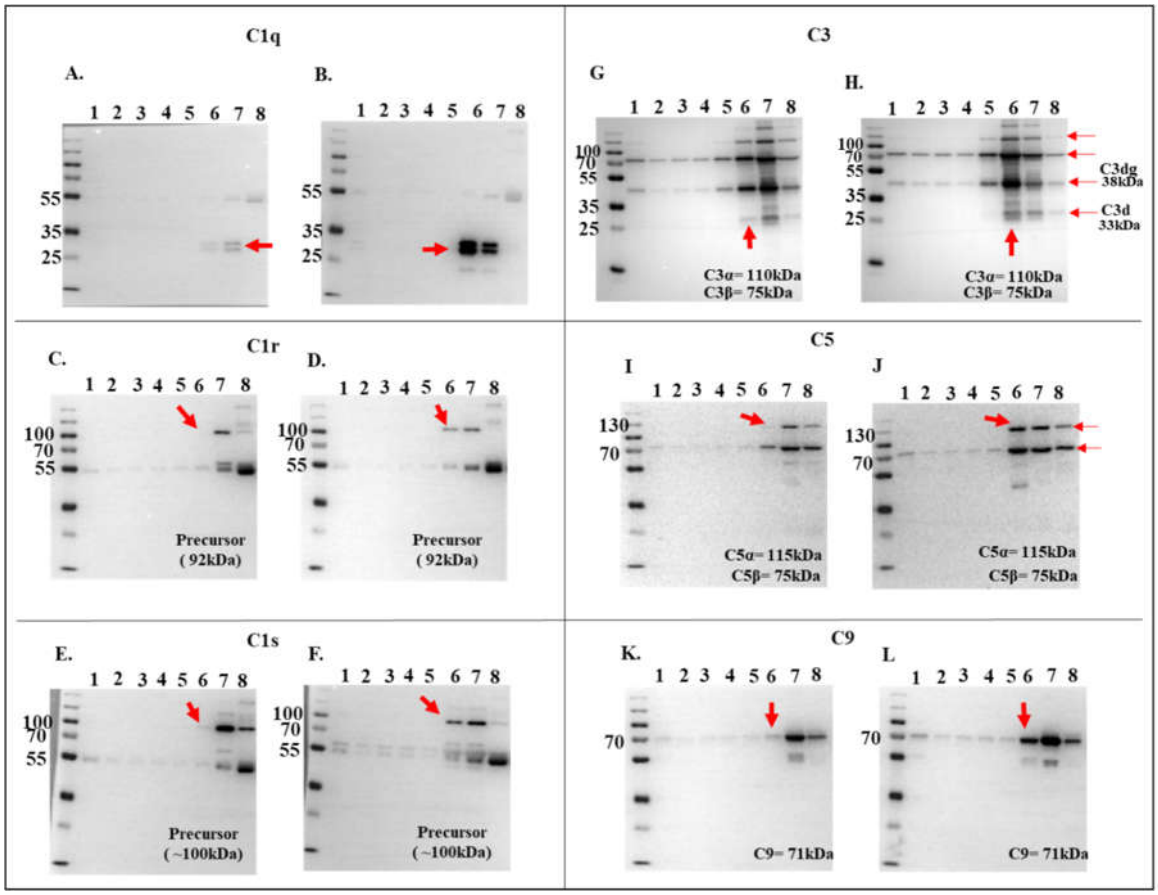

Figure 5. Validation of complement protein and r*Ixs*CRT interactions via western blotting analysis. To confirm the interactions observed in LCMS/MS analysis (referenced in Figure 3), DiffPOP fractions were subjected to standard western blotting using antibodies specific to complement proteins: C1q, C1r, C1s, C3, C5, and C9, as indicated. Unique binding patterns between NHS control and NHS + r*Ixs*CRT are indicated by red arrowheads. Panels A, C, E, G, I, and K, depict immunoblots of NHS-only samples, while panels B, D, F, H, J, and L represent immunoblots of NHS + r*Ixs*CRT samples.

To definitively ascertain the binding of complement proteins to r*Ixs*CRT, we employed Dynabeads™ His-Tag magnetic beads for the pull-down of r*Ixs*CRT and plasma protein complexes (Figure 6). Subsequently, these complexes underwent the standard western blotting analysis using antibodies similar to those utilized in Figure 5. Our rigorous analysis unequivocally validated the association of complement C1 complex proteins (C1q, C1r, and C1s), as well as intermediate complement proteins C3, C5, and C9, with r*Ixs*CRT. Specifically, distinct signals were detected in the r*Ixs*CRT and NHS pull-down samples, while being conspicuously absent in the NHS-only control (Figure 6). These findings provide robust evidence of the direct interaction between r*Ixs*CRT and key components of the host complement system, further elucidating the molecular mechanisms underlying tick-host interactions.

 doi:10.20944/preprints202404.1648.v1

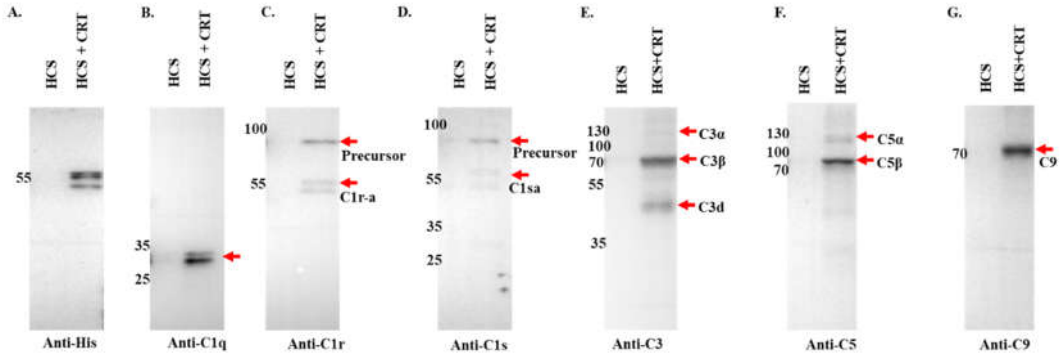

Figure 6. Pull down assay validates r*Ixs*CRT binding of complement proteins. Affinity purified r*Ixs*CRT bound onto His specific magnetic beads (Dynabeads™) was used to pull down complement proteins from human complement serum (HCS). The beads were washed and the eluted protein complexes were subjected to western blotting analysis using antibodies to histidine tag (A) and complement proteins C1q (B), C1r (C), C1s (D), C3 (E), C5 (F), C9 (G). In all the panels (A-G), HCS is the human complement serum which was eluted from the empty beads i.e., without the bait protein (r*Ixs*CRT) and HCS+r*Ixs*CRT denotes the human complement proteins which were pulled down and eluted from the beads loaded with r*Ixs*CRT. Red arrowheads denote the detected complement proteins at their expected molecular weight size (kDa).

To further validate differential fractionation and pull-down data (Figure 5 and 6), conventional ELISA was used to confirm r*Ixs*CRT binding of complement proteins. We coated ELISA plates with r*Ixs*CRT and then incubated with NHS. Uncoated wells were used as negative control. As shown, we observed significantly high antibody binding in wells that were coated with r*Ixs*CRT than uncoated control wells. Our data confirm that r*Ixs*CRT bound the C1 complex proteins (C1q, C1r and C1s) and intermediate complement proteins, C3, and C5 but not activated C3, and the C5b-C9 (or membrane attack complex) (Figure 7).

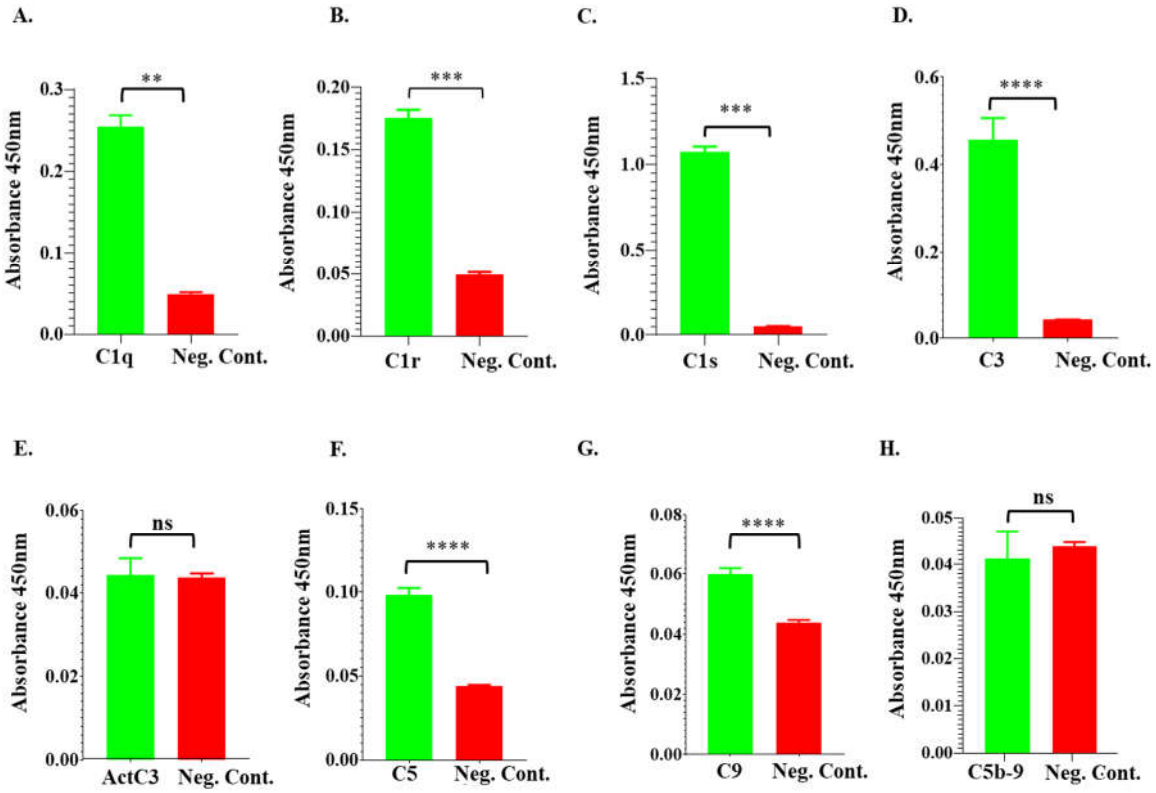

 doi:10.20944/preprints202404.1648.v1

Figure 7. ELISA analysis demonstrates r*Ixs*CRT binding of complement proteins. High Binding ELISA plates coated with affinity purified r*Ixs*CRT (250ng) was incubated with normal human serum (NHS) followed by antibodies to C1q (A), C1r (B), C1s (C), C3 (D), activated C3 (E), C5 (F), C9 (G), and C5b-9 or MAC (H) antibodies. Y-axis denotes the absorbance measured at A_{450nm} which reflects to the intensity of the specific antibody binding to r*Ixs*CRT. Non-coated well blocked with 1% BSA was incubated with NHS and used as negative control (Neg. Cont.). Data represents mean ± SEM of 3 biological replicate. For statistical analysis, t-test was performed on GraphPad Prism 9 and ** represents $p < 0.01$; *** represents $p < 0.001$, **** represents $p < 0.0001$, ns represents not significant.

3.4. rIxsCRT Moderately Inhibits Membrane Attack Complex (MAC) Deposition via Lectin Complement Cascade but Does Not Protect B. burgdorferi from Complement Killing

Prompted by findings that r*Ixs*CRT bound complement proteins, we investigated the effect of this protein on activation of the complement system using the WIESLAB® complement system kit, which allows for independent assessment of the three complement activation pathways. Our data show that r*Ixs*CRT inhibited deposition of the complement membrane attack complex (MAC) by 40% via the Mannan-Binding Lectin complement activation pathway but not via the classical and alternative complement activation pathways (Figure 8). We next evaluated if r*Ixs*CRT could protect complement sensitive *B. burgdorferi* strain (B314/pBBE22luc) against killing by complement. Our data showed that pre-incubating serum with r*Ixs*CRT did not protect complement sensitive strain from killing by complement (not shown).

Prompted by findings in our differential precipitation analysis that r*Ixs*CRT interacted with blood clotting factor XII and fibrin clot formation pathways, we investigated the effect of this protein on blood clotting using the recalcification time assay. This analysis showed that r*Ixs*CRT did not affect blood clotting (not shown).

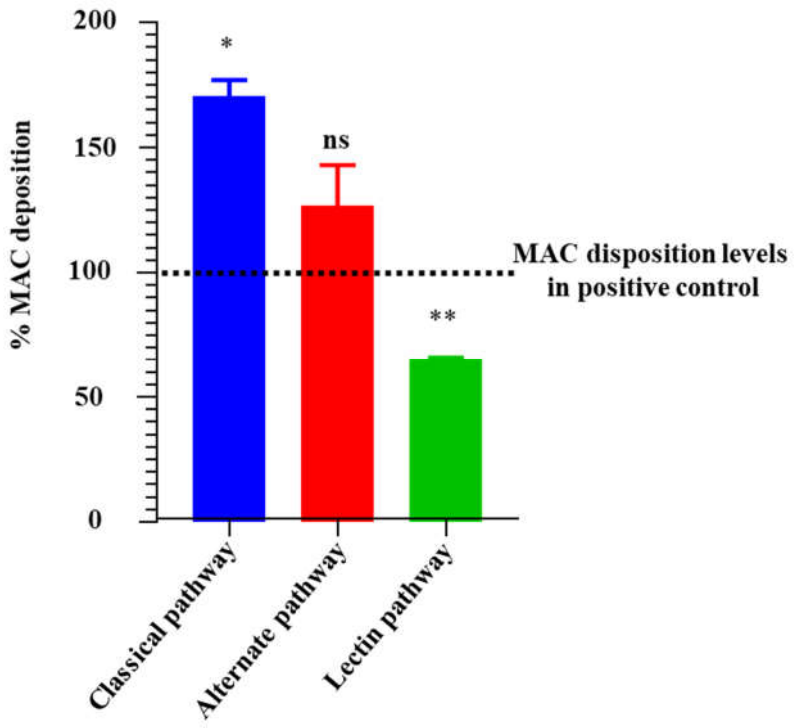

Figure 8. r*Ixs*CRT apparently enhances membrane attack complex (MAC) deposition in classical pathway and alternate pathway but inhibits MAC deposition in lectin pathway. Wieslab® Complement System Kit (Svar Life Science AB, Sweden) was used to detect the effects of r*Ixs*CRT on MAC deposition via Classical pathway, Alternative pathways and Lectin pathway as described in materials and methods. In brief, r*Ixs*CRT (4μM) was incubated with NHS (provided with the kit) at

 doi:10.20944/preprints202404.1648.v1

37°C for 30min and then added to wells pre-coated with the antibody to MAC. Diluent and kit provided reagent served as negative and positive control respectively. After washing, the conjugate and substrate were added according to the manufacturer instructions for each kit. NC is negative control and NHS is normal human serum used as positive control. % MAC deposition (Y-axis) was calculated as mentioned in methodology section and the MAC deposition in positive control was represented as 100% (denoted by black dotted line). Data is presented as deposited MAC ± SEM calculated from 3 biological replicates. Statistical significance was determined by student's t-test in GraphPad Prism 9. * Represents $p \leq 0.05$, ** represents $p \leq 0.01$ and ns represents not significant.

3.5. rIxsCRT Promotes Borrelia burgdorferi Growth in Culture

Next, we have investigated the effects of r*Ixs*CRT on growth of *B. burgdorferi* in culture. In this study we have observed that the *B. burgdorferi* (10^5 cells per mL) grown with r*Ixs*CRT showed significant elevation in the growth rate of *B. burgdorferi* (Figure 9). The spirochetes were quantified by Petroff-Hausser Chamber and processed for genomic DNA extraction for FlaB gene quantification by qPCR. Both of these analyses showed that r*Ixs*CRT promoted *B. burgdorferi* growth in culture by more than 10 folds at its log phase (Figure 9A and 9B).

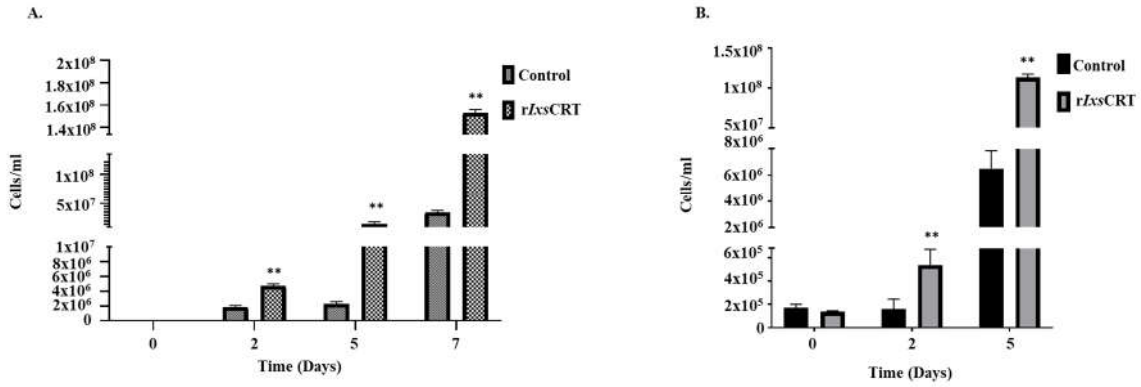

Figure 9. r*Ixs*CRT promotes the growth of *B. burgdorferi* in culture. *B. burgdorferi* cultured in presence of r*Ixs*CRT (indicated concentration) were sampled at days 0, 2, 5 and 7. (A) In triplicate, cells were quantified by manual counts on Petroff-Hausser Chamber and quantified using the following formula: number of cells/mL = Average of cells counted in all chambers x dilution factor x 50,000. (B) *B. burgdorferi* was quantified by qPCR using the genomic DNA of the *B. burgdorferi* and *flaB* primers. For ELISA, student's t-test was used for statistical analysis on GraphPad Prism 9 and p value ≤ 0.05 (denoted by **) is considered as significant value for 3 biologicals replicates. .

3.6. B. burgdorferi Infected I. scapularis Feeding Elicit High IgG Level to rIxsCRT in Rabbits

In an earlier study, we identified r*Ixs*CRT as one of the tick saliva proteins that were abundantly secreted by *B. burgdorferi*-infected *I. scapularis* nymphs [17]. Consistent with the dynamic secretion pattern of r*Ixs*CRT protein, rabbits that were fed upon by *B. burgdorferi*-infected ticks exhibited significantly higher levels of IgG antibodies reacting to r*Ixs*CRT compared to rabbits fed upon by uninfected ticks (Figure 10A-D).

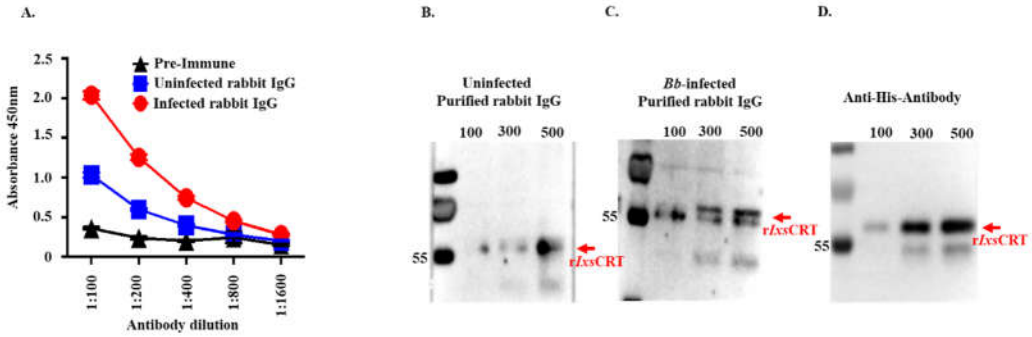

 doi:10.20944/preprints202404.1648.v1

Figure 10. One-time exposure of rabbits to *B. burgdorferi* infected *I. scapularis* nymphs triggers high IgG antibody levels to r*Ixs*CRT. (A) Affinity purified r*Ixs*CRT (250 ng) was subjected to standard ELISA using serially diluted purified IgG of rabbits that were fed on for a single time by uninfected (blue line graph) and *B. burgdorferi* infected (red line graph) *I. scapularis* nymph ticks. Black line graph represents pre-immune IgG binding that was used for negative control. (B-D) Various quantities of affinity purified r*Ixs*CRT (100, 300, and 500 ng) was subjected to western blotting analysis using purified IgG from rabbits that were fed on for a single time by uninfected (B) and *B. burgdorferi* infected ticks (C) as well as the antibody to the histidine tag that served as positive control (D).

4. Discussion

Calreticulin (CRT) is a well-known protein which was originally identified as calcium ion binding protein localized to the sarcoplasmic reticulum in rabbits [50]. It was originally believed to retain in endoplasmic reticulum and functions as molecular chaperon and Ca^{2+} homeostasis [51]. However, in ixodid ticks it was surprisingly found to lack endoplasmic reticulum (ER) retention signal (KDEL) [23] and it has been confirmed to be injected into the host during tick feeding [17] and it is currently used as the biomarker for tick bites [18]. The findings in this study elucidates the role of CRT in tick infestation dynamics. We demonstrate that rabbits infested only once against both uninfected or *B. burgdorferi* infected *I. scapularis* nymph feeding exhibited elevated antibody titers against recombinant *I. scapularis* calreticulin (r*Ixs*CRT), affirming its potential as a reliable marker for tick bites. These findings not only underscore the multifaceted functions of CRT but also highlight its practical application in diagnosing tick infestations.

Studies in mammals have reported a plethora of CRT functions including calcium storage, cell proliferation, ion binding, apoptosis, and cell differentiation [51]. Likewise, other parasite CRT was linked to parasite evasion of the complement through sequestration of complement proteins and blocking the blood clotting system through binding of blood clotting factor Xa [52]. While further validation studies are needed, our differential precipitation and LC-MS/MS analyses data showing r*Ixs*CRT interacted with multiple pathways indicate that tick CRT is likely involved with regulating several functions at the tick feeding site. Consistent with published studies that reported tick and other parasite CRT interactions with complement and blood clotting pathway proteins [53,54], r*Ixs*CRT differentially co-precipitated with proteins associated these two pathways. Since the tick must evade both complement and blood clotting host defenses to successfully feed and transmit tick borne disease pathogens [55], the findings in this study suggest a role for *Ixs*CRT in mediating tick evasion of host defense functions.

Evasion of the complement system by *B. burgdorferi* is critical in the pathogenesis of this spirochete [56], and thus we were curious to further explore interactions between r*Ixs*CRT and complement proteins. Published studies have reported that tick CRT could bind to C1q, one of the 3 subunits (C1q, C1 and C1s) of the C1 complex[27,31]. This study has provided new insights into functions of tick CRT by showing that r*Ixs*CRT binds to all three C1 complex complement proteins (C1q, C1r, and C1s) and to multiple intermediate complement proteins including C3, C5, C6, C7, C8, C9, complement factor I, and complement factor H. Further, our pull-down and ELISA analyses data demonstrates that although r*Ixs*CRT directly binds C1 complex proteins, intermediate, and late complement proteins, it does not bind the activated C5b-9 or the membrane attack complex (MAC).

Complement cascades are activated via 3 different pathways, classical, alternative, and mannose-binding lectin (MBL). Activation of the classical complement pathway starts with C1q binding onto microbe surface of antigen which in turn activates 2 subunits of C1 complex (C1r and C1s) [28,57]. Likewise, the MBL pathway is activated by the binding of MBL and ficolins to microbial surface oligosaccharides on microbe surfaces [58]. Lastly, the alternative pathway is activated by spontaneous hydrolysis of the internal C3 thioester bond and binding of properdin to proteins, lipids, and carbohydrate on microbe surfaces [59]. The activation of the 3 pathways culminates in activation of the C3 convertase which leads to C5 convertase, which reacts with complement proteins C6, C7, C8, and C9 to form C5b-9 or MAC. It is notable that despite binding of the C1 complex proteins, C3, C5, and C9, r*Ixs*CRT moderately blocked MAC deposition via the MBL pathway but not via the

 doi:10.20944/preprints202404.1648.v1

classical and alternative pathways. In our study we have noticed an increase in the MAC deposition in presence of r*Ixs*CRT in classical and alternate pathway, which is consistent with our previous study that showed that increasing amounts of recombinant *A. americanum* tick CRT led to deposition of high amounts of MAC [31]. The fact that tick CRT binds complement proteins but moderately affects MAC deposition via the MBL pathway but not via the 2 other pathways is interesting and warrants additional investigations. The complement sensitive strain of *B. burgdorferi* (B314/pBBE22luc) has been utilized to study inhibitors of the complement system in *B. burgdorferi* pathogenesis [37,60]. Our findings that r*Ixs*CRT did not rescue complement sensitive strain from complement killing may be explained by the fact that r*Ixs*CRT had modest impact in the MBL pathway and no effect in classical and alternate pathway. We speculate that the protective effects of *Ixs*CRT against complement killing of *B. burgdorferi* nullified by its lack of effect against classical and alternative activation pathways of complement despite reducing MAC deposition via the MBL pathway.

We have previously shown that *B. burgdorferi* infected *I. scapularis* nymphs highly secrete *Ixs*CRT during the 48-72 feeding time points aligning with high *B. burgdorferi* transmission events after the tick has fed for more than 48 h [15,17]. This suggested that *B. burgdorferi* might directly interact with *Ixs*CRT to promote its colonization of the host. It is interesting to note that supplementing the BSK-II media with r*Ixs*CRT enhanced the growth pattern of *B. burgdorferi* under in vitro conditions. We speculate that exposure to *Ixs*CRT triggers the rapid growth of *B. burgdorferi* at the site of its transmission and thus facilitating the establishment of local dermal infection that precedes colonization of secondary organs [61].

This study adds to our knowledge and raises questions warranting further investigations on the role of tick CRT in feeding and transmission of *B. burgdorferi* by ticks. It is particularly interesting that although *Ixs*CRT bound the C1 complex complement proteins, it did not block deposition of the MAC via the classical pathway. We speculate that in the complex environment of host skin, the *Ixs*CRT protein may serve as decoy that deviates the activation surface of complement from *B. burgdorferi* to *Ixs*CRT. Our DiffPOP data revealed that, r*Ixs*CRT interacted with extracellular matrix proteins such as collagen. It is possible that at the tick feeding site, native CRT bound to exposed extracellular matrix proteins could serve as the site of complement activation and in the process deviating complement attack of transmitted *B. burgdorferi.*

Supplementary Materials: The following supporting information can be downloaded at: www.mdpi.com/xxx/s1, Supplementary Table S1: Precipitation Buffer Volume for Differential Fractionation. This table provides details on the amount of precipitation buffer (in mL) added to the reaction to obtain the precipitate for the differential fractionation process. Supplementary Table S2: LC-MS/MS Analysis of Fractions 1-5. This table presents the results of LC-MS/MS analysis conducted on fractions 1-5 obtained from the differential precipitation assay of r*Ixs*CRT with normal human plasma. The data is provided in Excel format. Supplementary Table S3: LC-MS/MS Analysis of Fraction 6. This table displays the results of LC-MS/MS analysis performed on fraction 6 obtained from the differential precipitation assay of r*Ixs*CRT with normal human plasma. The data is presented in Excel format. Supplementary Table S4: Reactome Analysis of Complete LCMS/MS Data. This table presents the results of Reactome analysis conducted on the complete LCMS/MS dataset obtained from the differential precipitation assay of r*Ixs*CRT with normal human plasma. The data is provided in Excel format.

Author Contributions: Conceived and designed the experiment: AM, MAA. Performed the experiment: MAA, TTN, THK. Analyzed the data: AM, MAA, TNN, THK, TKK. Wrote the paper: MAA, AM.

Funding: This research was supported by National Institutes of Health grants (AI093858, AI074789, AI138129, and AI119873) to AM.

Acknowledgments: The author would like to thank Drs. Jon T Skare and Alexandra D Powell-Pierce for providing the *B. burgdorferi* strains and sharing their complement sensitivity assay protocols. We are grateful to Dr. Klaudia Kocurek for helping us to acquire LC-MS/MS data with assistance of the Mass Spectrometry Facility at the Department of Chemistry.

Conflicts of Interest: The authors declare no conflicts of interest.

References

1. Sosa, J.P.; Ferreira Caceres, M.M.; Agadi, K.; Pandav, K.; Mehendale, M.; Mehta, J.M.; Go, C.C.; Matos, W.F.; Guntipalli, P.; Belizaire, M.E. Diseases Transmitted by the Black-Legged Ticks in the United States: A Comprehensive Review of the Literature. *Cureus* **2021**, *13*, e17526, doi:10.7759/cureus.17526.
2. Wolf, M.J.; Watkins, H.R.; Schwan, W.R. Ixodes scapularis: Vector to an Increasing Diversity of Human Pathogens in the Upper Midwest. *WMJ* **2020**, *119*, 16-21.
3. Guzman, N.; Yarrarapu, S.N.S.; Beidas, S.O. Anaplasma Phagocytophilum. In *StatPearls*; Treasure Island (FL) ineligible companies. Disclosure: Siva Naga Yarrarapu declares no relevant financial relationships with ineligible companies. Disclosure: Sary Beidas declares no relevant financial relationships with ineligible companies., 2023.
4. Krause, P.J. Human babesiosis. *Int J Parasitol* **2019**, *49*, 165-174, doi:10.1016/j.ijpara.2018.11.007.
5. Piantadosi, A.; Solomon, I.H. Powassan Virus Encephalitis. *Infect Dis Clin North Am* **2022**, *36*, 671-688, doi:10.1016/j.idc.2022.03.003.
6. Wikel, S.K. Ticks and Tick-Borne Infections: Complex Ecology, Agents, and Host Interactions. *Vet Sci* **2018**, *5*, doi:10.3390/vetsci5020060.
7. Pritt, B.S.; Fernholz, E.C.; Replogle, A.J.; Kingry, L.C.; Sciotto, M.P.; Petersen, J.M. Borrelia mayonii - A cause of Lyme borreliosis that can be visualized by microscopy of thin blood films. *Clin Microbiol Infect* **2022**, *28*, 823-824, doi:10.1016/j.cmi.2021.07.023.
8. Pritt, B.S.; Respicio-Kingry, L.B.; Sloan, L.M.; Schriefer, M.E.; Replogle, A.J.; Bjork, J.; Liu, G.; Kingry, L.C.; Mead, P.S.; Neitzel, D.F.; et al. Borrelia mayonii sp. nov., a member of the Borrelia burgdorferi sensu lato complex, detected in patients and ticks in the upper midwestern United States. *Int J Syst Evol Microbiol* **2016**, *66*, 4878-4880, doi:10.1099/ijsem.0.001445.
9. Stevenson, B. The Lyme disease spirochete, Borrelia burgdorferi, as a model vector-borne pathogen: insights on regulation of gene and protein expression. *Curr Opin Microbiol* **2023**, *74*, 102332, doi:10.1016/j.mib.2023.102332.
10. Hook, S.A.; Jeon, S.; Niesobecki, S.A.; Hansen, A.P.; Meek, J.I.; Bjork, J.K.H.; Dorr, F.M.; Rutz, H.J.; Feldman, K.A.; White, J.L.; et al. Economic Burden of Reported Lyme Disease in High-Incidence Areas, United States, 2014-2016. *Emerg Infect Dis* **2022**, *28*, 1170-1179, doi:10.3201/eid2806.211335.
11. Obaid, M.K.; Islam, N.; Alouffi, A.; Khan, A.Z.; da Silva Vaz, I., Jr.; Tanaka, T.; Ali, A. Acaricides Resistance in Ticks: Selection, Diagnosis, Mechanisms, and Mitigation. *Front Cell Infect Microbiol* **2022**, *12*, 941831, doi:10.3389/fcimb.2022.941831.
12. Nauen, R.; Stumpf, N.; Elbert, A.; Zebitz, C.P.; Kraus, W. Acaricide toxicity and resistance in larvae of different strains of Tetranychus urticae and Panonychus ulmi (Acari: Tetranychidae). *Pest Manag Sci* **2001**, *57*, 253-261, doi:10.1002/ps.280.
13. Paucar-Quishpe, V.; Perez-Otanez, X.; Rodriguez-Hidalgo, R.; Cepeda-Bastidas, D.; Perez-Escalante, C.; Grijalva-Olmedo, J.; Enriquez, S.; Arciniegas-Ortega, S.; Sandoval-Travez, L.; Benavides-Erazo, B.; et al. An economic evaluation of cattle tick acaricide-resistances and the financial losses in subtropical dairy farms of Ecuador: A farm system approach. *PLoS One* **2023**, *18*, e0287104, doi:10.1371/journal.pone.0287104.
14. Trager, W. Acquired Immunity to Ticks. *The Journal of Parasitology* **1939**, *25*, 57-81, doi:https://doi.org/10.2307/3272160.
15. Kim, T.K.; Tirloni, L.; Bencosme-Cuevas, E.; Kim, T.H.; Diedrich, J.K.; Yates, J.R., 3rd; Mulenga, A. Borrelia burgdorferi infection modifies protein content in saliva of Ixodes scapularis nymphs. *BMC Genomics* **2021**, *22*, 152, doi:10.1186/s12864-021-07429-0.
16. Kim, T.K.; Tirloni, L.; Pinto, A.F.M.; Diedrich, J.K.; Moresco, J.J.; Yates, J.R., 3rd; da Silva Vaz, I., Jr.; Mulenga, A. Time-resolved proteomic profile of Amblyomma americanum tick saliva during feeding. *PLoS Negl Trop Dis* **2020**, *14*, e0007758, doi:10.1371/journal.pntd.0007758.
17. Kim, T.K.; Tirloni, L.; Pinto, A.F.; Moresco, J.; Yates, J.R., 3rd; da Silva Vaz, I., Jr.; Mulenga, A. Ixodes scapularis Tick Saliva Proteins Sequentially Secreted Every 24 h during Blood Feeding. *PLoS Negl Trop Dis* **2016**, *10*, e0004323, doi:10.1371/journal.pntd.0004323.
18. Alarcon-Chaidez, F.; Ryan, R.; Wikel, S.; Dardick, K.; Lawler, C.; Foppa, I.M.; Tomas, P.; Cushman, A.; Hsieh, A.; Spielman, A.; et al. Confirmation of tick bite by detection of antibody to Ixodes calreticulin salivary protein. *Clin Vaccine Immunol* **2006**, *13*, 1217-1222, doi:10.1128/CVI.00201-06.
19. Ferreira, C.A.; Da Silva Vaz, I.; da Silva, S.S.; Haag, K.L.; Valenzuela, J.G.; Masuda, A. Cloning and partial characterization of a Boophilus microplus (Acari: Ixodidae) calreticulin. *Exp Parasitol* **2002**, *101*, 25-34, doi:10.1016/s0014-4894(02)00032-2.
20. Jaworski, D.C., Simmen, F.A., Lamoreaux, W., Coons, L.B., Muller, M.T., Needham, G.R. A secreted calreticulin protein in ixodid tick (Amblyomma americanum) saliva. *Journal of Insect Physiology* **1995**, *41*, 369-375, doi:10.1016/0022-1910(94)00107-R.
21. Oladiran, A.; Belosevic, M. Trypanosoma carassii calreticulin binds host complement component C1q and inhibits classical complement pathway-mediated lysis. *Dev Comp Immunol* **2010**, *34*, 396-405, doi:10.1016/j.dci.2009.11.005.

 doi:10.20944/preprints202404.1648.v1

22. Lu, Y.C.; Weng, W.C.; Lee, H. Functional roles of calreticulin in cancer biology. *Biomed Res Int* **2015**, *2015*, 526524, doi:10.1155/2015/526524.
23. Deborah C. Jaworski, F.A.S., William Lamoreaux, Lewis B.Coons, Mark T.Muller, Glen R.Needham. A secreted calreticulin protein in ixodid tick (Amblyomma americanum) saliva. *Journal of Insect Physiology* **1995**, *41*, 369-375, doi:https://doi.org/10.1016/0022-1910(94)00107-R.
24. Suchitra, S.; Joshi, P. Characterization of Haemonchus contortus calreticulin suggests its role in feeding and immune evasion by the parasite. *Biochim Biophys Acta* **2005**, *1722*, 293-303, doi:10.1016/j.bbagen.2004.12.020.
25. Suchitra, S.; Anbu, K.A.; Rathore, D.K.; Mahawar, M.; Singh, B.P.; Joshi, P. Haemonchus contortus calreticulin binds to C-reactive protein of its host, a novel survival strategy of the parasite. *Parasite Immunol* **2008**, *30*, 371-374, doi:10.1111/j.1365-3024.2008.01028.x.
26. Sanders, M.L.; Glass, G.E.; Nadelman, R.B.; Wormser, G.P.; Scott, A.L.; Raha, S.; Ritchie, B.C.; Jaworski, D.C.; Schwartz, B.S. Antibody levels to recombinant tick calreticulin increase in humans after exposure to Ixodes scapularis (Say) and are correlated with tick engorgement indices. *Am J Epidemiol* **1999**, *149*, 777-784, doi:10.1093/oxfordjournals.aje.a009887.
27. Sanders, M.L.; Jaworski, D.C.; Sanchez, J.L.; DeFraites, R.F.; Glass, G.E.; Scott, A.L.; Raha, S.; Ritchie, B.C.; Needham, G.R.; Schwartz, B.S. Antibody to a cDNA-derived calreticulin protein from Amblyomma americanum as a biomarker of tick exposure in humans. *Am J Trop Med Hyg* **1998**, *59*, 279-285, doi:10.4269/ajtmh.1998.59.279.
28. Ferreira, V.; Valck, C.; Sanchez, G.; Gingras, A.; Tzima, S.; Molina, M.C.; Sim, R.; Schwaeble, W.; Ferreira, A. The classical activation pathway of the human complement system is specifically inhibited by calreticulin from Trypanosoma cruzi. *J Immunol* **2004**, *172*, 3042-3050, doi:10.4049/jimmunol.172.5.3042.
29. Vaithilingam, A.; Teixeira, J.E.; Miller, P.J.; Heron, B.T.; Huston, C.D. Entamoeba histolytica cell surface calreticulin binds human c1q and functions in amebic phagocytosis of host cells. *Infect Immun* **2012**, *80*, 2008-2018, doi:10.1128/IAI.06287-11.
30. Radulovic, Z.M.; Kim, T.K.; Porter, L.M.; Sze, S.H.; Lewis, L.; Mulenga, A. A 24-48 h fed Amblyomma americanum tick saliva immuno-proteome. *BMC Genomics* **2014**, *15*, 518, doi:10.1186/1471-2164-15-518.
31. Kim, T.K.; Ibelli, A.M.; Mulenga, A. Amblyomma americanum tick calreticulin binds C1q but does not inhibit activation of the classical complement cascade. *Ticks Tick Borne Dis* **2015**, *6*, 91-101, doi:10.1016/j.ttbdis.2014.10.002.
32. Mulenga, A.; Kim, T.K.; Ibelli, A.M. Deorphanization and target validation of cross-tick species conserved novel Amblyomma americanum tick saliva protein. *Int J Parasitol* **2013**, *43*, 439-451, doi:10.1016/j.ijpara.2012.12.012.
33. Ryan, B.J.; Kinsella, G.K. Differential Precipitation and Solubilization of Proteins. *Methods Mol Biol* **2017**, *1485*, 191-208, doi:10.1007/978-1-4939-6412-3_10.
34. Nguyen, T.T.; Kim, T.H.; Bencosme-Cuevas, E.; Berry, J.; Gaithuma, A.S.K.; Ansari, M.A.; Kim, T.K.; Tirloni, L.; Radulovic, Z.; Moresco, J.J.; et al. A tick saliva serpin, IxsS17 inhibits host innate immune system proteases and enhances host colonization by Lyme disease agent. *PLoS Pathog* **2024**, *20*, e1012032, doi:10.1371/journal.ppat.1012032.
35. Croft, D.; O'Kelly, G.; Wu, G.; Haw, R.; Gillespie, M.; Matthews, L.; Caudy, M.; Garapati, P.; Gopinath, G.; Jassal, B.; et al. Reactome: a database of reactions, pathways and biological processes. *Nucleic Acids Res* **2011**, *39*, D691-697, doi:10.1093/nar/gkq1018.
36. Bencosme-Cuevas, E.; Kim, T.K.; Nguyen, T.T.; Berry, J.; Li, J.; Adams, L.G.; Smith, L.A.; Batool, S.A.; Swale, D.R.; Kaufmann, S.H.E.; et al. Ixodes scapularis nymph saliva protein blocks host inflammation and complement-mediated killing of Lyme disease agent, Borrelia burgdorferi. *Front Cell Infect Microbiol* **2023**, *13*, 1253670, doi:10.3389/fcimb.2023.1253670.
37. Garcia, B.L.; Zhi, H.; Wager, B.; Hook, M.; Skare, J.T. Borrelia burgdorferi BBK32 Inhibits the Classical Pathway by Blocking Activation of the C1 Complement Complex. *PLoS Pathog* **2016**, *12*, e1005404, doi:10.1371/journal.ppat.1005404.
38. Gulliani, G.L.; Hyun, B.H.; Litten, M.B. Blood recalcification time. A simple and reliable test to monitor heparin therapy. *Am J Clin Pathol* **1976**, *65*, 390-396, doi:10.1093/ajcp/65.3.390.
39. Fanning, J.P.; Dubeau, A.M. The whole blood recalcification clotting time. A suggested simple and reliable method for monitoring heparin therapy. *J Maine Med Assoc* **1974**, *65*, 211, 213.
40. Pahl, A.; Kuhlbrandt, U.; Brune, K.; Rollinghoff, M.; Gessner, A. Quantitative detection of Borrelia burgdorferi by real-time PCR. *J Clin Microbiol* **1999**, *37*, 1958-1963, doi:10.1128/JCM.37.6.1958-1963.1999.
41. Richard, G. Autosomal Recessive Congenital Ichthyosis. In *GeneReviews((R))*, Adam, M.P., Feldman, J., Mirzaa, G.M., Pagon, R.A., Wallace, S.E., Bean, L.J.H., Gripp, K.W., Amemiya, A., Eds.; Seattle (WA), 1993.
42. Akiyama, M. ABCA12 mutations and autosomal recessive congenital ichthyosis: a review of genotype/phenotype correlations and of pathogenetic concepts. *Hum Mutat* **2010**, *31*, 1090-1096, doi:10.1002/humu.21326.
43. Akiyama, M. The roles of ABCA12 in epidermal lipid barrier formation and keratinocyte differentiation. *Biochim Biophys Acta* **2014**, *1841*, 435-440, doi:10.1016/j.bbalip.2013.08.009.

44. Akiyama, M.; Sugiyama-Nakagiri, Y.; Sakai, K.; McMillan, J.R.; Goto, M.; Arita, K.; Tsuji-Abe, Y.; Tabata, N.; Matsuoka, K.; Sasaki, R.; et al. Mutations in lipid transporter ABCA12 in harlequin ichthyosis and functional recovery by corrective gene transfer. *J Clin Invest* **2005**, *115*, 1777-1784, doi:10.1172/JCI24834.
45. Wu, L.; Li, Y.; Song, Y.; Zhou, D.; Jia, S.; Xu, A.; Zhang, W.; You, H.; Jia, J.; Huang, J.; et al. A recurrent ABCC2 p.G693R mutation resulting in loss of function of MRP2 and hyperbilirubinemia in Dubin-Johnson syndrome in China. *Orphanet J Rare Dis* **2020**, *15*, 74, doi:10.1186/s13023-020-1346-4.
46. Deroux, A.; Boccon-Gibod, I.; Fain, O.; Pralong, P.; Ollivier, Y.; Pagnier, A.; Djenouhat, K.; Du-Thanh, A.; Gompel, A.; Faisant, C.; et al. Hereditary angioedema with normal C1 inhibitor and factor XII mutation: a series of 57 patients from the French National Center of Reference for Angioedema. *Clin Exp Immunol* **2016**, *185*, 332-337, doi:10.1111/cei.12820.
47. Clark, E.A.; Giltiay, N.V. CD22: A Regulator of Innate and Adaptive B Cell Responses and Autoimmunity. *Front Immunol* **2018**, *9*, 2235, doi:10.3389/fimmu.2018.02235.
48. Hong, K.; Nishiyama, M.; Henley, J.; Tessier-Lavigne, M.; Poo, M. Calcium signalling in the guidance of nerve growth by netrin-1. *Nature* **2000**, *403*, 93-98, doi:10.1038/47507.
49. Xiong, Z.; Wang, Q.; Li, W.; Huang, L.; Zhang, J.; Zhu, J.; Xie, B.; Wang, S.; Kuang, H.; Lin, X.; et al. Platelet-Derived Growth Factor-D Activates Complement System to Propagate Macrophage Polarization and Neovascularization. *Front Cell Dev Biol* **2021**, *9*, 686886, doi:10.3389/fcell.2021.686886.
50. Ostwald, T.J.; MacLennan, D.H. Isolation of a high affinity calcium-binding protein from sarcoplasmic reticulum. *J Biol Chem* **1974**, *249*, 974-979.
51. Michalak, M.; Corbett, E.F.; Mesaeli, N.; Nakamura, K.; Opas, M. Calreticulin: one protein, one gene, many functions. *Biochem J* **1999**, *344 Pt 2*, 281-292.
52. Kuwabara, K.; Pinsky, D.J.; Schmidt, A.M.; Benedict, C.; Brett, J.; Ogawa, S.; Broekman, M.J.; Marcus, A.J.; Sciacca, R.R.; Michalak, M.; et al. Calreticulin, an antithrombotic agent which binds to vitamin K-dependent coagulation factors, stimulates endothelial nitric oxide production, and limits thrombosis in canine coronary arteries. *J Biol Chem* **1995**, *270*, 8179-8187, doi:10.1074/jbc.270.14.8179.
53. Ramirez-Toloza, G.; Aguilar-Guzman, L.; Valck, C.; Ferreira, V.P.; Ferreira, A. The Interactions of Parasite Calreticulin With Initial Complement Components: Consequences in Immunity and Virulence. *Front Immunol* **2020**, *11*, 1561, doi:10.3389/fimmu.2020.01561.
54. Esperante, D.; Flisser, A.; Mendlovic, F. The many faces of parasite calreticulin. *Front Immunol* **2023**, *14*, 1101390, doi:10.3389/fimmu.2023.1101390.
55. Simo, L.; Kazimirova, M.; Richardson, J.; Bonnet, S.I. The Essential Role of Tick Salivary Glands and Saliva in Tick Feeding and Pathogen Transmission. *Front Cell Infect Microbiol* **2017**, *7*, 281, doi:10.3389/fcimb.2017.00281.
56. Skare, J.T.; Garcia, B.L. Complement Evasion by Lyme Disease Spirochetes. *Trends Microbiol* **2020**, *28*, 889-899, doi:10.1016/j.tim.2020.05.004.
57. Dunkelberger, J.R.; Song, W.C. Complement and its role in innate and adaptive immune responses. *Cell Res* **2010**, *20*, 34-50, doi:10.1038/cr.2009.139.
58. Beltrame, M.H.; Catarino, S.J.; Goeldner, I.; Boldt, A.B.; de Messias-Reason, I.J. The lectin pathway of complement and rheumatic heart disease. *Front Pediatr* **2014**, *2*, 148, doi:10.3389/fped.2014.00148.
59. Harboe, M.; Mollnes, T.E. The alternative complement pathway revisited. *J Cell Mol Med* **2008**, *12*, 1074-1084, doi:10.1111/j.1582-4934.2008.00350.x.
60. van Dam, A.P.; Oei, A.; Jaspars, R.; Fijen, C.; Wilske, B.; Spanjaard, L.; Dankert, J. Complement-mediated serum sensitivity among spirochetes that cause Lyme disease. *Infect Immun* **1997**, *65*, 1228-1236, doi:10.1128/iai.65.4.1228-1236.1997.
61. Hyde, J.A. Borrelia burgdorferi Keeps Moving and Carries on: A Review of Borrelial Dissemination and Invasion. *Front Immunol* **2017**, *8*, 114, doi:10.3389/fimmu.2017.00114.